Journal of Neurochemistry
Lippincott Williams & Wilkins, Inc., Philadelphia

Identification and Characterization of Nuclear Factor κB Binding Sites in the Murine *bcl-x* Promoter

J. N. Glasgow, *T. Wood, and J. R. Perez-Polo

*Department of Human Biological Chemistry and Genetics and *Sealy Center for Molecular Science, University of Texas Medical Branch, Galveston, Texas, U.S.A.*

Abstract: Signal transduction pathways that mediate neuronal commitment to apoptosis involve the nuclear factor κB (NF-κB) transcription factor. Bcl-X_L is a potent regulator of apoptosis in the CNS and is highly expressed in the developing and adult brain. We identified three putative NF-κB DNA binding sequences clustered upstream of the brain-specific transcription start site in the upstream promoter region. Recombinant p50/p50 and NF-κB proteins from nuclear extracts bound to these sites as determined by electrophoretic mobility shift assay and biotin-oligonucleotide/streptavidin affinity assays. NF-κB overexpression, coupled with *bcl-x* promoter/reporter assays using a series of murine *bcl-x* promoter and deletion mutants, has identified the downstream 1.1 kb of the *bcl-x* promoter as necessary for basal promoter activity and induction by NF-κB. The mutagenic removal of NF-κB binding sites individually or in combination revealed altered response patterns to p49/p65 and p50/p65 overexpression. These results support the hypothesis that NF-κB can act to enhance Bcl-X_L expression via highly selective interactions, where NF-κB binding and *bcl-x* promoter activation are dependent on both DNA binding site sequence and NF-κB subunit composition. Our data suggest that molecular events associated with NF-κB promote regulation of neuronal apoptosis in the developing or injured CNS. **Key Words:** Nuclear factor κB—*bcl-x*—Apoptosis—Transcription—Promoter.
J. Neurochem. **75,** 1377–1389 (2000).

In addition to its fundamental role during development, neuronal apoptosis may be involved in the loss of specific neuronal populations in the CNS as a result of trauma, ischemia, age-associated neurodegenerative diseases, and normal aging (Oppenheim, 1991; Raff, 1992). Although many signals that induce apoptosis are known, less is known about the distinct intracellular effectors responsible for regulating commitment to apoptosis.

Several distinct protein families with diverse functions control various stages of the cell death program. The Bcl-2 family of apoptosis effector molecules with cell death inhibiting or promoting activities includes the antiapoptotic proteins Bcl-2, Bcl-x_L, and Bcl-w and their proapoptotic counterparts Bax, Bcl-x_S, and Bad (Cleary et al., 1986; Tsujimoto and Croce, 1986; Boise et al., 1993; Yang et al., 1995; Gibson et al., 1996).

Consistent with the role of Bcl-2 family proteins in determining cell fate, these proteins are subject to a complex system of regulation. Bcl-2 family members are controlled at the level of phosphorylation (Zha et al., 1996; Ito et al., 1997), proteolysis (Cheng et al., 1997; Gross et al., 1999), subcellular localization and/or redistribution (Hsu et al., 1997; Wolter et al., 1997), and transcription. These regulatory actions may serve to alter concentrations of active Bcl-2 family molecules at critical locations within the cell, especially the mitochondria. Consistent with this idea, manipulation of levels of these proteins via gene transfection and/or antisense oligonucleotides suggests that ratios of proapoptotic to antiapoptotic Bcl-2 family proteins determine the sensitivity or resistance of cells to various apoptotic stimuli.

The *bcl-x* gene is unique in that it can give rise to proapoptotic Bcl-x_S and antiapoptotic Bcl-x_L proteins via differential splicing of *bcl-x* mRNA (Boise et al., 1993). Bcl-x_L, but not Bcl-x_S, is highly expressed throughout the developing and postnatal CNS (Gonzalez-Garcia et al., 1994, 1995; Frankowski et al., 1995) and is a dominant inhibitor of apoptosis during development and postnatal life. In contrast to *bcl-2* (−/−) mice, *bcl-x* (−/−) mice die at embryonic day 13 and show massive cell death of neurons and hematopoietic progenitor cells (Motoyama et al., 1995; Michaelidis et al., 1996). Bcl-x_L prevents apoptosis of sympathetic neuron cell cultures following growth factor deprivation (Frankowski et al., 1995). Furthermore, Bcl-x_L overexpression protects mo-

Received April 18, 2000; revised manuscript received June 5, 2000; accepted June 12, 2000.

Address correspondence and reprint requests to Dr. J. R. Perez-Polo at Department of Human Biological Chemistry and Genetics, University of Texas Medical Branch, 301 University Boulevard, Galveston, TX 77555-0652, U.S.A. E-mail: jperezpo@utmb.edu

Abbreviations used: AP-1, activator protein-1; CMV, cytomegalovirus; EMSA, electrophoretic mobility shift assay; gsu, gel shift unit; HSV, herpes simplex virus; NF-κB, nuclear factor κB; RSV, Rous sarcoma virus; SDS-PAGE, sodium dodecyl sulfate–polyacrylamide gel electrophoresis; TK, thymidine kinase.

tor neurons from axotomy-induced apoptosis and promotes neuronal survival following hypoxia–ischemia injury in the hippocampus and other brain areas (Chen et al., 1997; Parsadanian et al., 1998).

The nuclear factor κB (NF-κB) family of transcription factors is involved in the regulation of genes regulating inflammation, response to infection and oxidative stress, and apoptosis (Beg et al., 1995; Sonenshein, 1997) and has recently been shown to be required for normal brain function (O'Neill and Kaltschmidt, 1997). This family is composed of five structurally related protein subunits: p49 (also called p52), p50, p65/RelA, c-Rel, and RelB, which form various dimers in multiple tissues. These proteins share a 300-amino acid region, the Rel homology domain, which is the structural basis for dimerization, DNA binding, and nuclear localization. In addition, the transcriptionally active p65/RelA, c-Rel, and RelB subunits contain a C-terminal acidic activation domain not present in the p49/p52 (referred to as p49 in this report) and p50 subunits. Thus, heterodimers containing p49 or p50 combined with p65, c-Rel, or RelB are capable of activating transcription (Liou and Baltimore, 1993). Despite this diversity, the active heterodimer p50/p65 is generally referred to as NF-κB.

Inactive NF-κB homo- and heterodimers are sequestered in the cytoplasm of cells complexed with one of several distinct inhibitory subunits, including IκB-α, IκB-β, and IκB-γ. IκB molecules are subject to phosphorylation, subsequent degradation, and release of active NF-κB on reception of signals that lead to NF-κB activation (Whiteside and Israel, 1997).

NF-κB dimers bind target gene regulatory regions through a wide variety of binding sites that generally match a 5′-GGGRNTY(C/T)C-3′ consensus (R = A or G, Y = C or T, N = any nucleotide). NF-κB achieves target gene specificity in part through preferential binding of different subunit combinations to numerous similar DNA sequences (Liou and Baltimore, 1993; Muller et al., 1993).

There is strong evidence that NF-κB participates in regulating apoptosis in numerous tissues, including the CNS (O'Neill and Kaltschmidt, 1997; Grilli and Memo, 1999). NF-κB may affect apoptosis in some tissue types by transcriptionally regulating genes that directly rescue cells (Foo and Nolan, 1999). In support of this hypothesis, there is evidence that NF-κB affects *bcl-x* gene expression in the nervous and immune systems, although the exact role of NF-κB in regulating this gene is far from clear (Dixon et al., 1997; Hettmann et al., 1999; Lee et al., 1999; Tamatani et al., 1999).

In this report we test the hypothesis that *bcl-x*, an antiapoptotic *bcl-2* gene family member, is a direct gene target of the transcription factor NF-κB. We identify two distinct NF-κB binding sites within the murine *bcl-x* promoter region that are responsible for NF-κB-mediated increases in *bcl-x* promoter activity in a PC12 cell transfection system.

MATERIALS AND METHODS

Sequence analysis

Human and mouse upstream promoter sequences (GenBank accession nos. D30746 and U78030, respectively) were analyzed for potential NF-κB binding sites and sequence alignment using the Genetics Computer Group Wisconsin version 9.0 Package. The *Tfsites* database was used as the search parameter for binding sites. Sequence alignment of mouse and human promoter sequences was performed using the GAP global fit alignment operation.

Cell culture

Rat pheochromocytoma PC12 cells were a gift of Lloyd A. Greene (Columbia University, New York, NY, U.S.A.) and were maintained in RPMI 1640 medium containing 5% fetal calf serum, 5% horse serum, and 1% penicillin/neomycin/streptomycin. Cells were maintained at 37°C in a humidified atmosphere containing 5% CO_2. Stock cultures were grown in 75-cm^2 tissue culture flasks, fed three times weekly, and divided once a week using vigorous shaking to dislodge cells from flasks.

Promoter activity transfection assays

Cells were plated in 32- or 60-mm-diameter plates and allowed to attach overnight. Cells were transfected at a 3:1 (wt/wt) liposome:DNA ratio using the DMRIE-C cationic liposome reagent and OPTI-MEM reduced-serum medium (GibcoBRL) according to the manufacturer's instructions. This ratio was determined as yielding the highest transfection efficiency (15–20%) as determined via pCMV-lacZ (where CMV represents cytomegalovirus) plasmid transfection and 5-bromo-4-chloro-3-indolyl β-D-galactopyranoside staining. For *bcl-x* promoter studies, 1 pmol of each respective *bcl-x* promoter/firefly luciferase construct was used per 10^6 cells. For *bcl-x* promoter/NF-κB coexpression, each transfection mixture also included 2 pmol of a single NF-κB expression vector (1 pmol each if two NF-κB vectors were used) or 2 pmol of pRSV-lacZ (where RSV represents Rous sarcoma virus) plasmid as a nonactivating control. Each transfection mixture also contained 0.01 pmol of pRL-TK (where TK represents thymidine kinase) *Renilla* luciferase expression plasmid (Promega) to control for transfection efficiency. DNA and liposome were mixed in OPTI-MEM. Cells were rinsed once in OPTI-MEM, and then 1 ml of DNA/liposome mixture was applied to the cells. Transfection time was 4 h, after which the liposome mixture was removed and replaced with complete medium. Transfected cells were collected after 24 h by rinsing with Tris-buffered saline and then lysed in 200 μl of Passive Lysis Buffer (Promega) by scraping. Lysates were kept on ice, cleared by microcentrifugation at 12,000 *g* for 5 min, transferred to fresh microfuge tubes, and stored at −80°C until used. Firefly and *Renilla* luciferase activities in 20 μl of lysate were assayed using the Dual Luciferase Assay System (Promega).

bcl-x promoter constructs

Expression vectors containing 3.2 kb (pGL2-3.2), the upstream 2.0 kb (pGL2-2.0), and downstream 1.1 kb (pGL2-1.1) of the murine *bcl-x* promoter region fused to a promoterless pGL2 firefly luciferase reporter were a generous gift of Dr. Gabriel Núñez (University of Michigan Medical School, Ann Arbor, MI, U.S.A.) (Grillot et al., 1997). All *bcl-x* promoter constructs do not contain nucleotides −1 to −90 with respect to the ATG. pGL2-0.6Left containing the upstream 600 bp of the 1.1-kb promoter in pGL2-1.1 was created by digesting pGL2-1.1 with *Hind*III and *Bgl*II, liberating the downstream

500 bp of the *bcl-x* promoter. The compatible cohesive ends of pGL2-0.6Left were ligated together with T4 ligase (Promega). pGL2-0.5Right was constructed by digesting pGL2-1.1 with *Xho*I and *Hind*III at the 5′ and 3′ ends, respectively, of the 1.1-kb insert, liberating the upstream 600 bp. The linear pGL2-0.5Right plasmid noncohesive ends were filled in with Klenow fragment, and the blunt ends were ligated together with T4 ligase (Life Technologies). Mutant *bcl-x* promoter constructs containing sequence replacements of NF-κB binding sites were created by the Sealy Center for Molecular Science Recombinant DNA Laboratory (University of Texas Medical Branch, Galveston, TX, U.S.A.) using the downstream 1.1 kb of the *bcl-x* promoter found in pGL2-1.1 as a template for mutagenesis. The three single-site replacement mutants were created by amplifying the 1.1-kb region of the *bcl-x* promoter by PCR using primers that replaced each NF-κB binding sequence with the 9-bp sequence 5′-AGATCAACT-3′. The replacement mutagenesis was performed using PCR-based strategy and the following mutagenic primers: for the *bcl-x* 1,145 mutation, 5′-GGTCTCCACTGTAGATCAACTGACCCTTCTTCC-3′ (sense) and 5′-GGAAGAAGGGTCAGTTGATCTACAGTGGAGACC-3′ (antisense); for the *bcl-x*-967 mutation, 5′-GCGGTGTTTGTGAGATCAACTCAGCATACGCCTC-3′ (sense) and 5′-GAGGCGTATGCTGAGTTGATCTCACAAACACCGC-3′ (antisense); and for the *bcl-x*-847 mutation, 5′-TTGAGATTCACTTAGATCAACTCTTTAGGGTTTCGG-3′ (sense) and 5′-GAAACCCTAAAGAGTTGATCTAAGTGAATCTCAAGG-3′ (antisense). The underlined sequence replaced each *bcl-x* NF-κB site in the final product. The double mutant *bcl-x*-847/967 1.1-kb promoter was created using the completed *bcl-x*-847 1.1-kb mutant promoter as a template for introducing the *bcl-x*-967 mutation. The finished *bcl-x*-847/-967 double mutant promoter was used as the template for the introduction of the *bcl-x*-1,145 mutation to form the triple mutant 1.1-kb promoter. All mutations and finished plasmid sequences were confirmed by DNA sequence analysis.

NF-κB and IκB-α expression vectors

The following reagents were obtained through the AIDS Research and Reference Reagent Program, Division of AIDS, NIAD, NIH: pRSV-NK-κB2 (p49), pRSV-NK-κB1 (p50), and pRSV-RelA (p65) NF-κB from Dr. Gary Nabel and Dr. Neil Perkins (Gorman et al., 1983; Schmid et al., 1991; Perkins et al., 1992; Duckett et al., 1993). These expression vectors contain cDNAs from human p49, p50, and RelA/p65 subunits of NF-κB under the transcriptional control of the RSV long terminal repeat. The pCMV4-IκB-α eukaryotic expression vector containing a FLAG epitope-tagged human IκB-α cDNA with alanine replacement at Ser^{32} and Ser^{36} was a generous gift of Dean Ballard (Vanderbilt University) (Brockman et al., 1995). The pRSV-lacZ control expression vector containing the *Escherichia coli lacZ* gene under the control of the RSV long terminal repeat (Mitchell et al., 1989) was a gift of Ronald Walter (Southwest Texas State University, San Marcos, TX, U.S.A.). The pRL-TK *Renilla* luciferase expression vector (Promega) was a gift of Dr. E. Aubrey Thompson (University of Texas Medical Branch, Galveston) NF-κB-Luc firefly luciferase reporter was obtained from Clontech.

Oligonucleotides

Unmodified complementary single-stranded oligonucleotides used in electrophoretic mobility shift assays (EMSA) were synthesized by Sigma-Genosys (The Woodlands, TX, U.S.A.). Chemically modified complementary single-stranded oligonucleotides containing a 5′ biotin molecule at the end of a 15-atom linker were synthesized by Synthegen (Houston, TX, U.S.A.). All single-stranded oligonucleotides were annealed in sterile TEN buffer (1 m*M* EDTA, 50 m*M* NaCl, and 10 m*M* Tris, pH 7.5) at a stock concentration of 2 μg/μl. The IgG-κB sequence was 5′-AGTTGAGGGGACTTTCCCAGGC-3′. The activator protein-1 (AP-1) sequence was 5′-CGCTTGATGACTCAGCCGGAA-3′. Oligonucleotides containing mouse genomic *bcl-x* NF-κB sequences included the NF-κB binding sequence and 6 bp of genomic 5′ and 3′ flanking sequences as follows: position *bcl-x*-1,145, 5′-CACTGTGGGAGCCCCGACCCT-3′; position *bcl-x*-967, 5′-TTTGTGGGGGGTCTCCAGCAT-3′; and position *bcl-x*-847, 5′-TCACTTGGAAGTCCCTTTAGG 3′. Transcription factor binding sequences within each oligonucleotide are underlined.

Preparation of nuclear extracts for EMSA analysis

PC12 cells were collected by scraping the Tris-buffered saline (pH 7.6) and pelleted by centrifugation at 800 *g*. Cell pellets were suspended in 500 μl of buffer containing 10 m*M* HEPES (pH 7.9), 10 m*M* KCl, 0.1 m*M* EDTA, 0.1 m*M* EGTA, 1.0 m*M* dithiothreitol, 0.5 m*M* phenylmethylsulfonyl fluoride, and the protease inhibitors antipain, chymostatin, pepstatin, and leupeptin at 2 μg/ml each. The pellets were kept on ice for 10 min, and 25 μl of a 10% solution of NP-40 was added. The cell lysate was centrifuged at 8,000 *g* for 2 min. The cleared cytosolic fraction was removed, and the pelleted nuclei were resuspended in 100 μl of buffer containing 20 m*M* HEPES (pH 7.9), 0.4 *M* NaCl, 1.0 m*M* EDTA, 1.0 m*M* EGTA, 1.0 m*M* dithiothreitol, 1.0 m*M* phenylmethylsulfonyl fluoride, and protease inhibitors as above. The nuclear suspension was shaken vigorously for 20 min at 4°C. The nuclear lysate was cleared by centrifugation at 13,000 *g* for 5 min at 4°C. Nuclear extracts were aliquoted and frozen at −80°C, and protein concentrations were determined by the BCA protein assay (Pierce).

Nuclear extract from 70Z/3 cells was a gift of Dr. Norbert K. Herzog (University of Texas Medical Branch, Galveston) and was prepared as described (Dyer and Herzog, 1995). In brief, 70Z/3 cells were treated with 10 μg/ml *Salmonella typhosa* lipopolysaccharide for 6 h. Cells were collected by centrifugation at 200 *g* for 5 min at 4°C. The cell pellet was resuspended in 100 μl of sucrose buffer 1 [0.32 *M* sucrose, 3 m*M* $CaCl_2$, 2 m*M* magnesium acetate, 0.1 m*M* EDTA, 10 m*M* Tris-HCl (pH 8.0), 0.1 m*M* dithiothreitol, 0.5 m*M* phenylmethylsulfonyl fluoride, and 0.5% (vol/vol) NP-40]/10^7 cells. The lysate was centrifuged at 500 *g* for 5 min at 4°C to pellet the nuclei, and the cytoplasm was transferred to a fresh tube. Nuclei were resuspended in low-salt buffer [20 m*M* HEPES (pH 7.9), 25% glycerol, 1.5 m*M* $MgCl_2$, 0.02 *M* KCl, 0.2 m*M* EDTA, 0.5 m*M* dithiothreitol, and 0.5 m*M* phenylmethylsulfonyl fluoride] at 20 μl/10^7 cells. Nuclei were extracted in high-salt buffer [20 m*M* HEPES (pH 7.9), 1.5 m*M* $MgCl_2$, 0.8 m*M* KCl, 0.2 m*M* EDTA, 1% NP-40, 0.5 m*M* dithiothreitol, and 0.5 m*M* phenylmethylsulfonyl fluoride] by slowly adding a volume equal to the low-salt buffer. Nuclear lysate was incubated with gentle mixing for 20 min at 4°C. Before the final centrifugation at 13,000 *g* for 15 min at 4°C, the nuclear lysate was diluted 1:2.5 with diluent buffer [25 m*M* HEPES (pH 7.6), 25% glycerol, 0.1 m*M* EDTA, 0.5 m*M* dithiothreitol, and 0.5 m*M* phenylmethylsulfonyl fluoride]. The final lysate was aliquoted and frozen at −80°C. Protein concentrations were determined as above.

EMSA

Oligonucleotides containing the three putative genomic binding sites and 6-bp flanking sequences and a positive control

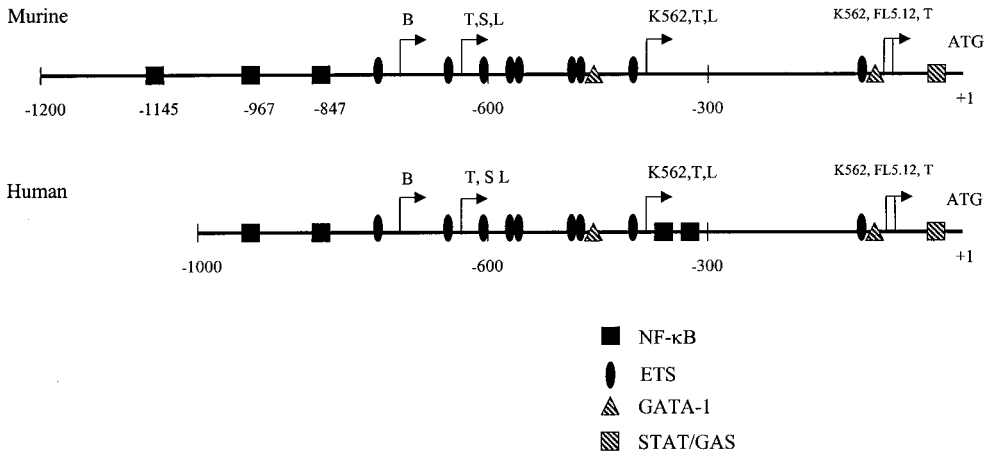

FIG. 1. Schematic representation of the murine (**upper**) and human (**lower**) *bcl-x* promoter regions. The diagram shows the highly conserved nature of the spatial arrangement of sequence elements in the two promoters. Putative binding sequences are shown only for transcription factors that have been suggested to activate the *bcl-x* promoter. Except for NF-κB binding sites, only binding sequences conserved between the mouse and human promoters are shown: interferon-γ activation site (GAS) motif for STAT1/5 interaction (▨) (Fujio et al., 1997; Silva et al., 1999); NF-κB binding sites (■) (Dixon et al., 1997; Lee et al., 1999; present study); Ets-family binding sites for Ets-2 (●) (Sevilla et al., 1999); and GATA motif for the GATA-1 transcription factor (△) (Grillot et al., 1997; Gregory et al., 1999). The NF-κB binding sequences in the murine promoter studied in this report are found at positions −847, −976, and −1,145 nucleotides upstream from the initiator codon ATG. Arrows indicate major transcription initiation start sites for murine brain (B), thymus (T), liver (L), spleen (S), and FL5.12 and K562 cells (Grillot et al., 1997).

oligonucleotide containing the IgG-κB NF-κB binding sequence were end-labeled with 2 μl of 4,000 Ci/mmol [γ-^{32}P]-ATP (ICN) and T4 polynucleotide kinase (Promega). Labeling efficiencies were consistent among different oligonucleotides as judged by examining free probe on EMSA autoradiographs. Labeled oligonucleotides were incubated for 30 min with 8 μg of 70Z/3 cell nuclear extract (gift of Dr. Norbert K. Herzog), 8 μg of PC12 cell nuclear extract, or 1 gel shift unit (gsu; 1 gsu is 95 ng of protein) human recombinant p50 (Promega). Binding reactions were in a 20-μl volume containing 10% glycerol, 50 m*M* KCl, 20 m*M* EDTA, 20 m*M* dithiothreitol, and 10 m*M* HEPES (pH 7.5) for 30 min at room temperature. Each reaction mixture also contained 1 μg of poly(dI–dC) as a competitor for nonspecific DNA-binding proteins. Competitive controls included 50-fold molar excess of unlabeled oligonucleotide. Supershift/immunodepletion assays contained 2 μg of p50 or p65 polyclonal antibody (Santa Cruz) incubated for 30 min in the reaction mixture before addition of labeled oligonucleotide. Binding reactions were subjected to 6% polyacrylamide electrophoresis at 120 V for 3 h at 4°C. Gels were dried under vacuum and exposed to x-ray film.

Microaffinity purification of NF-κB proteins

Oligonucleotides containing binding sequences of NF-κB were synthesized and chemically modified to contain a 5′ biotin molecule on the end of a 15-atom linker (Synthegen). Four picomoles (final concentration, 2.0×10^{-7} *M*) of duplex biotin-labeled oligonucleotide was incubated with 1 gsu of the human recombinant p50 subunit of NF-κB (Promega) in a 20-μl volume containing 12% glycerol, 1 μg of poly(dI–dC), 0.05% NP-40, 50 m*M* KCl, 200 μ*M* EDTA, 2.5 m*M* dithiothreitol, and 10 m*M* HEPES (pH 7.6) for 45 min at room temperature. For competition studies, excess unlabeled oligonucleotide was also added at 5.0×10^{-8}, 1.0×10^{-7}, 2.0×10^{-7}, 4.0×10^{-7}, 8.0×10^{-7}, 2.0×10^{-6}, and 4.0×10^{-6} *M*. NF-κB proteins bound to biotin-oligonucleotides were precipitated by addition of 6 μl of a 50% (vol/vol) slurry of streptavidin-agarose beads (Pierce). After 30 min of agitation at 4°C, the streptavidin–biotin–protein–DNA complex was pelleted by centrifugation at 1,000 *g* in a microfuge. The agarose bead/oligonucleotide/protein complexes were then washed three times in 10 volumes of 1× binding buffer. Proteins were then removed from the oligonucleotides by addition of 2× sodium dodecyl sulfate–polyacrylamide gel electrophoresis (SDS-PAGE) sample buffer and then boiled for 5 min. The entire binding reaction was electrophoresed on a 10% SDS-PAGE gel and then transferred to a polyvinylidene membrane for western analysis. Western analysis detection of NF-κB proteins was achieved with a primary antibody against the p50 subunit of NF-κB (Santa Cruz). Primary antibodies were diluted 1:20,000, and the secondary horseradish peroxidase-conjugated antibody was used at a 1:5,000 dilution. Protein bands were detected via ECL (Amersham) and exposure to x-ray film. Specific protein bands were quantitated using AlphaEase version 3.24 image analysis software. Band density measurements from each binding reaction mixture were expressed as a percentage of values from binding reaction mixtures that contained no unlabeled oligonucleotide.

Statistical analysis

Differences between multiple, large groups were analyzed by the Kruskal–Wallis nonparametric ANOVA for comparison of groups with statistically different SDs followed by Dunn's post test. Values of $p < 0.05$ between groups were considered significant.

RESULTS

Identification of NF-κB sites in the *bcl-x* promoter

Following sequence analysis of the murine *bcl-x* gene, we identified three putative NF-κB binding sequences in the 5′-regulatory region of the murine *bcl-x* gene beginning at positions −847 (5′-GGAAGTCCC-3′), −967

(5′-GGGGGTCTCC-3′), and −1,145 (5′-GGGAGC-CCC-3′) nucleotides from the initiator ATG (Fig. 1). These sites bear significant homology to the 5′-GGGRN-TY(C/T)C-3′ consensus NF-κB sequence (Lenardo et al., 1989). Unconfirmed NF-κB sites similar to murine *bcl-x*-847 and identical to *bcl-x*-967 sites are conserved in the human *bcl-x* promoter region (Fig. 1).

NF-κB binds to sequences in the *bcl-x* 5′-regulatory region

To determine if these sequences were authentic NF-κB binding sites, double-stranded oligonucleotides making up each putative NF-κB binding site and 12 bp of genomic flanking sequence were tested via EMSA for binding of NF-κB proteins. First, each *bcl-x* NF-κB sequence was tested for binding to purified human recombinant p50/p50 NF-κB homodimers. As shown in Fig. 2, p50/p50 binds to the three *bcl-x* sequences (lanes 4, 7, and 9) and to the IgG-κB-positive control sequence (lane 1). Bound p50 was displaced by a 50-fold molar excess of unlabeled oligonucleotide (lanes 2, 5, 8, and 11) but not by a 50-fold molar excess of an unlabeled, unrelated oligonucleotide containing the AP-1 consensus sequence (lanes 3, 6, 9, and 12). Binding of p50/p50 to the *bcl-x* NF-κB sequences was less robust than to the IgG-κB control sequence. Whereas p50/p50 showed relatively strong binding to *bcl-x*-847 and *bcl-x*-967 sequences, it did not bind as strongly to the *bcl-x*-1,145 sequence (compare Fig. 2, lanes 7 and 10 with lane 4).

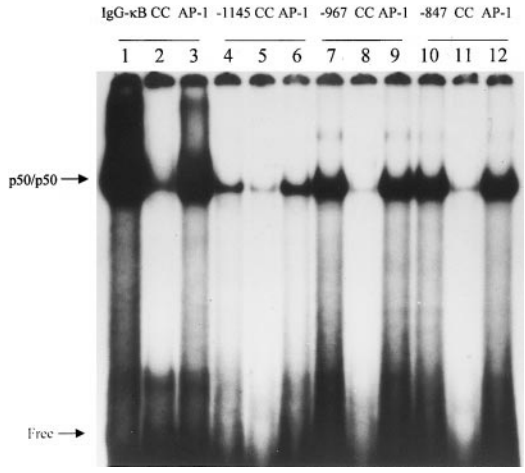

FIG. 2. Human recombinant p50/p50 binds specifically to oligonucleotides containing NF-κB binding sites from the murine *bcl-x* promoter. Shown is a representative EMSA analysis of 1 gsu per lane of human recombinant p50 (Promega). Lanes 1–3, positive control IgG-κB sequence (Sen and Baltimore, 1986); lanes 4–6, murine *bcl-x*-1,145 sequence; lanes 7–9, murine *bcl-x*-967 sequence; and lanes 10–12, murine *bcl-x*-847 sequence. Lanes 2, 5, 8, and 11, competitive control (CC) with 50-fold excess unlabeled oligonucleotide; lanes 3, 6, 9, and 12, competitive control containing 50-fold excess unlabeled AP-1 consensus sequence oligonucleotide. The upper arrow indicates the position of the specific p50/oligonucleotide complex. The lower arrow indicates free probe.

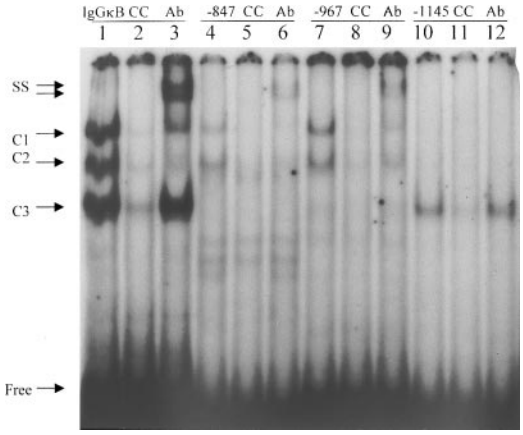

FIG. 3. Nuclear NF-κB proteins bind *bcl-x* promoter sequences. Shown is EMSA analysis of 70Z/3 pre-B cell nuclear extracts and p50 supershift/immunodepletion analysis. Supershift analysis with a p50 antibody (Ab) identified complex C1 as p50/p65 and complex C2 as primarily p50/p50 NF-κB-containing complexes (p65 supershift not shown). Lanes 1–3, positive control IgG-κB sequence; lanes 4–6, *bcl-x*-847 sequence; lanes 7–9, *bcl-x*-967 sequence; and lanes 10–12, *bcl-x*-1,145 sequence. Competitive control (CC) lanes 2, 5, 8, and 11 contained a 50-fold excess of unlabeled oligonucleotide. Lanes 3, 6, 9, and 12 contained 1 μl of p50 Ab. Each lane received 6 μg of nuclear protein extract from 70Z/3 cells treated with lipopolysaccharide for 6 h.

To evaluate the ability of the *bcl-x* NF-κB sites to bind nuclear NF-κB proteins, we incubated nuclear extracts from lipopolysaccharide-treated 70Z/3 cells with labeled oligonucleotides containing the three different *bcl-x* NF-κB sequences. 70Z/3 cells were widely used as a pre-B cell model to study inducible NF-κB activity and exhibit p50/p50 and p50/p65 dimers of NF-κB via EMSA (Liou et al., 1994). As shown in Fig. 3, lanes 4 and 7, two complexes, C1 and C2, were formed with nuclear extracts from 70Z/3 cells treated with lipopolysaccharide and the *bcl-x*-847 and *bcl-x*-967 NF-κB binding sites. Identical complexes were also formed with a positive control IgG-κB oligonucleotide (Fig. 3, lane 1). Both C1 and C2 bands were abolished by addition of 50-fold excess unlabeled oligonucleotide and were identified as NF-κB-containing complexes by immunodepletion/supershift analysis using an anti-p50 antibody that resulted in two separate supershifted species (Fig. 3, lanes 3, 6, and 9). Complex C2 is a p50/p50 homodimer, as judged by elimination of the complex with the p50 antibody, and complex C1 contains p50 and is composed primarily of p50/p65 as judged by immunodepletion/supershift analysis (p65 immunodepletion/supershift not shown). Complex C3 is the protein RPB-Jκ, a transcriptional repressor that binds to a 5′-TGGGAA-3′ consensus sequence present in some NF-κB binding sites (Norbert K. Herzog, personal communication). There was no appreciable NF-κB binding to position −1,145. Taken together, these data show that among the three putative NF-κB sites in the *bcl-x* 5′-regulatory region, only *bcl-x*-847 and *bcl-x*-967 NF-κB sites significantly bind to NF-κB proteins.

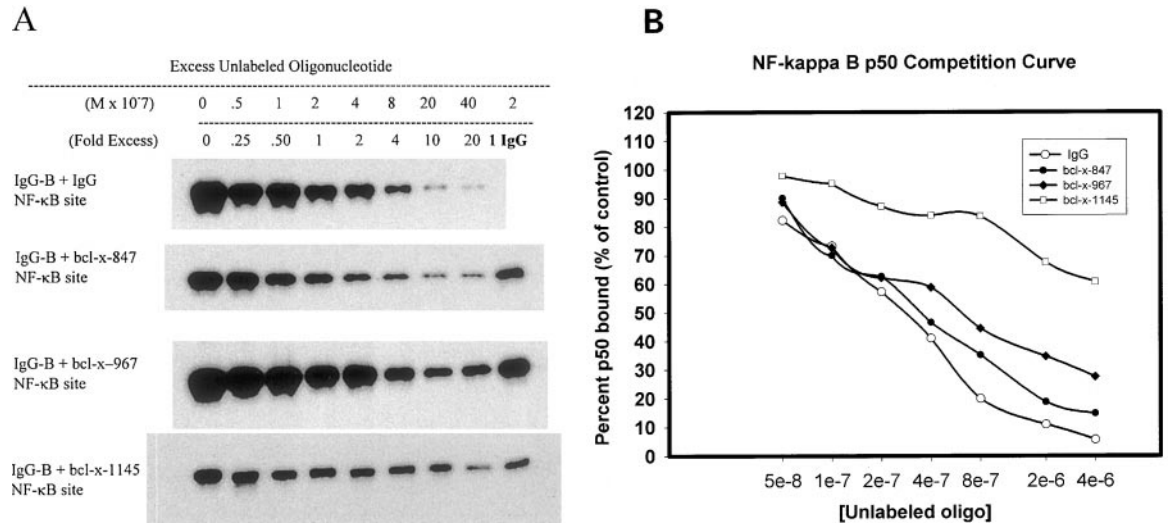

FIG. 4. Competitive binding studies demonstrate relative binding affinities of recombinant p50 for each of the three *bcl-x* NF-κB binding sites compared with the IgG-κB sequence. **A:** Western blot analysis of p50 binding reactions to biotin-labeled IgG-κB sequence oligonucleotides in the presence of increasing unlabeled IgG-κB or *bcl-x* NF-κB site oligonucleotides. Fold excess unlabeled oligonucleotide is indicated at the top, along with the concentration of the unlabeled oligonucleotide in the binding reaction. Biotin-labeled IgG-κB oligonucleotide was 2×10^{-7} *M* in each DNA binding reaction. Groups containing unlabeled *bcl-x* sequence oligonucleotides contained one control reaction with equimolar IgG-κB, indicated by 1 IgG. **B:** Each curve represents the binding of human recombinant p50 to biotin-labeled IgG-κB oligonucleotide (2×10^{-7} *M*) in the presence of increasing unlabeled oligonucleotide containing the IgG-κB sequence (○), *bcl-x*-847 sequence (●), *bcl-x*-967 sequence (◆), or *bcl-x*-1,145 sequence (□). NF-κB p50 protein bound to biotin-labeled oligonucleotides was precipitated and analyzed by western blot analysis (see Materials and Methods). Points on each curve are the average of two values from independent experiments expressed as percentages of internal control binding reactions that contained p50, biotin-labeled IgG-κB oligonucleotide, and no unlabeled oligonucleotide.

To characterize further the apparent difference in affinity for NF-κB, we determined the relative binding affinity of p50/p50 for the three different *bcl-x* NF-κB sites. Recombinant NF-κB p50/p50 was incubated with 2.0×10^{-7} *M* biotin-labeled IgG-κB oligonucleotide, and p50/oligonucleotide complexes were precipitated by addition of streptavidin-agarose beads. The NF-κB proteins were then eluted from the oligonucleotides with 2× SDS-PAGE sample buffer and subjected to SDS-PAGE followed by western blot analysis. Figure 4 shows the effect of increasing concentration of unlabeled IgG-κB and *bcl-x* NF-κB binding site oligonucleotides on p50/p50 binding to the biotin-IgG-κB sequence. Competition curves of p50/p50 binding were obtained from measuring band densities of p50 western blot bands (Fig. 4A). Band density values were expressed as percentages of band density values from control binding reaction mixtures that received no unlabeled oligonucleotide (Fig. 4B). Addition of an equimolar amount (2.0×10^{-7} *M*) of unlabeled IgG-κB oligonucleotide decreased binding of p50/p50 to the biotin-IgG oligonucleotides to 55% of control. The *bcl-x*-847 and *bcl-x*-967 sequences competed for p50/p50 binding similarly but to a lesser extent than the IgG-κB sequence, requiring up to a threefold excess ($\sim 6.0 \times 10^{-7}$ *M*) of unlabeled oligonucleotide to decrease binding to 50% of the control value. The *bcl-x*-1,145 sequence showed very low affinity for p50/p50, only slightly competing for p50/p50 binding at a 20-fold molar excess (4.0×10^{-6} *M*). An unlabeled AP-1 consensus oligonucleotide did not compete for p50/p50 binding even at a 20-fold molar excess (data not shown). These data are consistent with the EMSA analyses in Figs. 2 and 3 that show that only *bcl-x*-847 and *bcl-x*-967 sequences strongly bind p50/p50 or p50/p65 NF-κB proteins.

The *bcl-x* promoter region spanning nucleotides −1,200 to −600 is important for NF-κB-mediated activation

To determine the effect of NF-κB proteins on the *bcl-x* promoter, we used *bcl-x* promoter constructs containing different regions of the 5′-regulatory region of the murine *bcl-x* gene fused upstream of the firefly luciferase reporter gene (Grillot et al., 1997). We chose to overexpress NF-κB subunits via eukaryotic expression vectors encoding the NF-κB subunits p49 (pRSVp49), p50 (pRSVp50), and p65 (pRSVp65) during transfections of the murine *bcl-x* promoter. The first step in establishing this NF-κB/*bcl-x* promoter transfection system as a means of describing a role for NF-κB in *bcl-x* transcriptional regulation was to test the NF-κB expression vectors for their ability to activate specific NF-κB-dependent transcription. PC12 cells (Greene and Tischler, 1976) were transfected with pNF-κB-Luc, a firefly luciferase reporter plasmid under the control of a NF-κB-dependent promoter containing four tandem NF-κB binding sites of sequence 5′-GGGAATTTCC-3′ fused to the herpes simplex virus (HSV) Tk minimal promoter (Clontech). pNF-κB-Luc was significantly activated by cotransfection with pRSVp65 and pRSVp50/pRSVp65

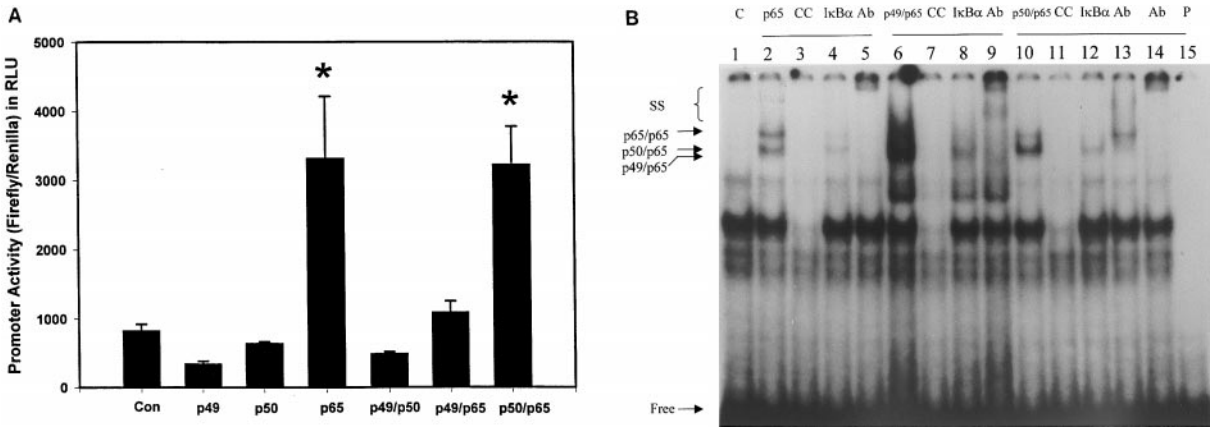

FIG. 5. Overexpression of NF-κB subunits in PC12 cells leads to increased DNA binding activity and NF-κB-dependent promoter activation. **A:** Promoter activity of the NF-κB-dependent firefly luciferase reporter plasmid pNF-κB-Luc cotransfected with expression vectors for NF-κB subunits. The control group (Con) received pRSV-*lacZ* in place of NF-κB expression vector(s) (see Materials and Methods). Promoter activity is expressed as relative light units (RLU) of firefly luciferase activity normalized to *Renilla* luciferase activity to control for any differences in transfection efficiency. Data are mean ± SD (bars) values for five cultures per group. $^*p < 0.001$ versus Con. **B:** EMSA analysis of nuclear extracts from PC12 cells transfected with pRSV-p65/RelA (lanes 2–5), pRSV-p49/pRSV-p65/RelA (lanes 6–9), or pRSV-p50/pRSV-p65/RelA (lanes 10–14). Lanes 4, 8, and 12 were cotransfected with pCMV-IκB-α. Lane 1 contains nuclear proteins from control (C) cells treated with liposomes only. Lane 15 contains only radiolabeled IgG-κB probe (P). Lanes 3, 7, and 11 are competitive control (CC) lanes containing 50-fold molar excess of unlabeled probe. Lanes 5, 9, and 13 contained 1 μl of p65 polyclonal antibody (Ab). Lane 14 contained 1 μl of p50 Ab. p49/p65, p50/p65, and p65/p65, NF-κB/oligonucleotide complexes are indicated by arrows. The lower arrow indicates free probe. Lanes 1–14 received 8 μg of nuclear extract. All lanes contained 0.2 pmol of labeled IgG-κB probe. The results are representative of three independent experiments.

but not significantly by pRSVp49/pRSVp65 (Fig. 5A). pNF-κB-Luc was not transcriptionally activated by pRSVp49, pRSVp50, or pRSVp49/pRSVp50. This subunit-specific pattern of NF-κB-dependent promoter activation is consistent with the established role of p65/RelA-containing NF-κB dimers as transcriptional activators (Perkins et al., 1992; Lin et al., 1995).

To establish further that the NF-κB overexpression model parallels physiologic nuclear localization, dimer formation, and IκB-α-mediated inhibition, we transfected PC12 cells with pRSVp49/pRSVp65 and pRSVp50/pRSVp65, with or without pCMV4-IκB-α, an expression vector encoding the mutant "superrepressor" form of the NF-κB inhibitory subunit IκB-α (Brockman et al., 1995). This mutant form of IκB-α contains serine to alanine changes at amino acid positions 32 and 36 and cannot be phosphorylated, the signal for IκB-α degradation and subsequent release of active NF-κB. EMSAs performed with nuclear extracts from transfected cells exhibited marked increases in specific NF-κB binding over control mock-transfected controls. Figure 5B shows the NF-κB binding profile of an IgG-κB probe to nuclear extracts from PC12 cells transfected with pRSVp65 alone (Fig. 5B, lanes 2–5). pRSVp49/pRSVp65 (Fig. 5B, lanes 6–9), or pRSVp50/pRSVp50 (Fig. 5B, lanes 10–14). Overexpression of pRSVp65 yielded two distinct bands, which were competed away by a 50-fold excess of unlabeled oligonucleotide and were supershifted by an anti-p65/RelA antibody (Fig. 5B, lanes 2, 3, and 5). The lower band migrated to the same position at the p50/p65 heterodimer in lane 10 and is likely p50/p65 formed with endogenous p50; we presume the upper band to be p65/p65 (Fig. 5B, lane 2). pRSVp49/pRSVp65 and pRSVp50/pRSVp65 transfection resulted in p49/p65 heterodimer (Fig. 5B, lane 6) and p50/p65 heterodimer (Fig. 5B, lane 10) complexes, which were specifically competed away by a 50-fold excess of unlabeled oligonucleotide (Fig. 5B, lanes 7 and 11) and supershifted by anti-p50 or anti-p65/RelA antibodies (Fig. 5B, lanes 9 and 14, respectively). It is notable that IκB-α cotransfection virtually eliminated shifted bands corresponding to p49/p65, p50/p65, and p65/p65 (Fig. 5B, lanes 4, 8, and 12). Similarly, EMSAs using nuclear extracts from cells transfected with pRSVp49 and pRSVp50, alone or in combination, yielded distinct homo- and heterodimers as determined by immunodepletion/supershift analysis (data not shown). The results in Fig. 5 establish that overexpression of NF-κB subunits does result in NF-κB-dependent transcriptional activation and nuclear localization of specific NF-κB heterodimers in PC12 cells.

EMSA analysis using *bcl-x*-847, -967, and -1,145 binding site oligonucleotides with nuclear extracts from cells transfected with p49/p65 or p50/p65 showed binding of p49/p65 and p50/p65 dimers to Bcl-x-967, as confirmed by immunodepletion/supershift analysis. However, we observed no appreciable binding to the *bcl-x*-847 or *bcl-x*-1,145 sequences using similar nuclear extracts (data not shown). Given our data showing that both p50/p50 and p50/p65 bind the *bcl-x*-847 sequence (Fig. 3), we were surprised that this sequence oligonucleotide did not bind p49/p65 or p50/p65 from transfected cells. That no NF-κB binding to the *bcl-x*-1,145 sequence was observed was consistent with our other results (Figs. 2–4).

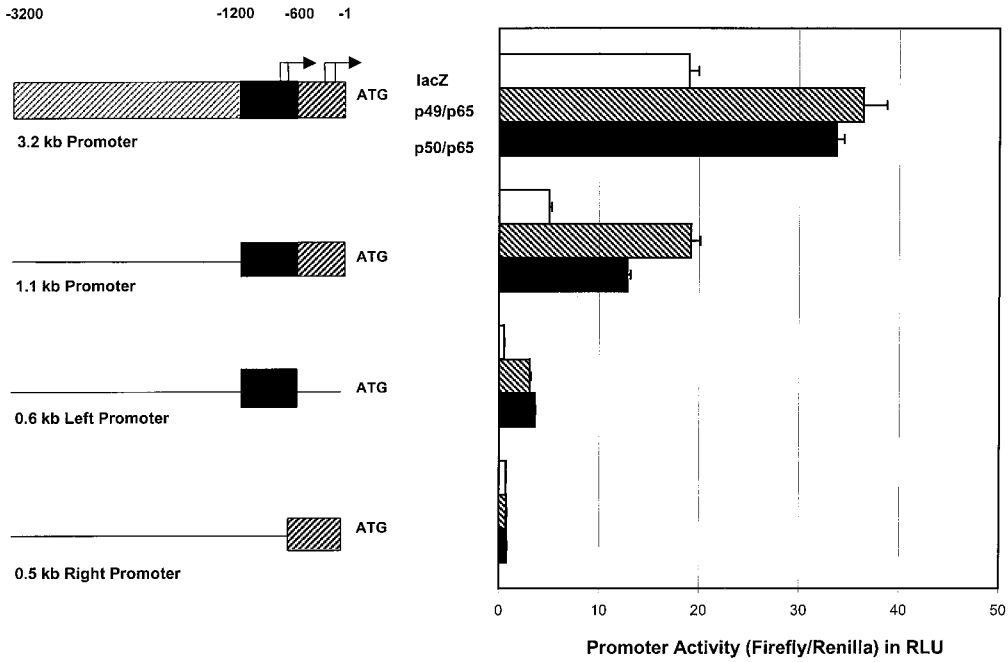

FIG. 6. Representative results of relative promoter activities of *bcl-x* promoter regions in the presence of pRSV-*lacZ* (□), p49/p65 (▨), and p50/p65 (■) overexpression in PC12 cells. The *bcl-x* promoter activity is expressed as relative light units (RLU) of firefly luciferase activity normalized to RLU of *Renilla* luciferase to control for any differences in transfection efficiency. The full-length *bcl-x* promoter construct pGL2-3.2 and each deletion mutant promoter are depicted on the left of each promoter's activity. Filled region in the *bcl-x* promoter indicates nucleotide positions −1,200 to −600 containing the three NF-κB sites. Transcription start sites are indicated by arrows. Data are mean ± SD (bars) values of six cultures per group. The results are representative of at least two independent experiments.

Based on our results indicating that there are at least two genuine NF-κB binding sites in the *bcl-x* promoter, we wanted to determine if overexpression of NF-κB proteins could activate the *bcl-x* promoter. We used a series of *bcl-x* promoter constructs containing 3.2 (pGL2-3.2), 1.1 (pGL2-1.1), 0.6 (pGL2-0.6Left), and 0.5 kb (pGL2-0.5Right) of the *bcl-x* promoter ligated into a promoterless luciferase reporter vector, pGL2-Basic, as described herein and elsewhere (Grillot et al., 1997). In brief, PC12 cells were transiently transfected with *bcl-x* promoter/firefly luciferase hybrid constructs with and without NF-κB expression vectors, and luciferase activity was determined 24 h posttransfection. All transfection data were normalized for transfection efficiency using pRL-TK, a *Renilla* luciferase expression vector driven by a minimal HSV-TK promoter (Promega). Sequence analysis of the HSV-TK promoter revealed no NF-κB binding sites, and transfection mixtures containing only pRL-TK and NF-κB expression vectors did not result in increased *Renilla* luciferase activity (data not shown).

We have observed inconsistent promoter activity during cotransfection experiments due to "promoter interference" between the experimental and normalization vectors. To eliminate this problem in our transfections, all transfection groups received equimolar amounts of RSV-driven NF-κB expression vector(s) or a control pRSV-*lacZ* expression vector in addition to the pRL-TK *Renilla* luciferase normalization vector.

Figure 6 shows representative results of relative basal promoter activity of the full-length 3.2-kb *bcl-x* promoter/enhancer and a 1.1-, 0.6-, and 0.5-kb promoter regions in PC12 cells. Elimination of the upstream 2.0-kb region from pGL2-3.2 resulted in a decrease in the basal promoter activity of pGL2-1.1. Basal activities of pGL2-0.6Left and pGL2-0.5Right were further decreased but remained ~10-fold higher than values in nontransfected controls (data not shown). Relative basal transcriptional activities of each promoter region in human K562 cells were qualitatively similar to those in rat PC12 cells (data not shown). Addition of pRSVp49/p65 or pRSVp50/p65 increased promoter activity of the 3.2-kb promoter construct approximately twofold over baseline control, and the pGL2-1.1 and pGL2-0.6Left promoter activities were increased between two- and sevenfold above their respective baseline controls. Cotransfection with pRSVp49, pRSVp50, or the combination of pRSVp49/pRSVp50 did not consistently alter promoter activity of pGL2-3.2 or pGL2-1.1 promoters compared with cotransfection with pRSV-*lacZ* (data not shown). The addition of pRSVp49/p65 or pRSVp50/p65 did not increase the promoter activity of pGL2-0.5Right, which does not contain *bcl-x*-847, *bcl-x*-967, or *bcl-x*-1,145 sequences but contains transcriptional start sites at positions −400 and −96 (Fig. 1). These data strongly suggest that the region of the *bcl-x* promoter spanning nu-

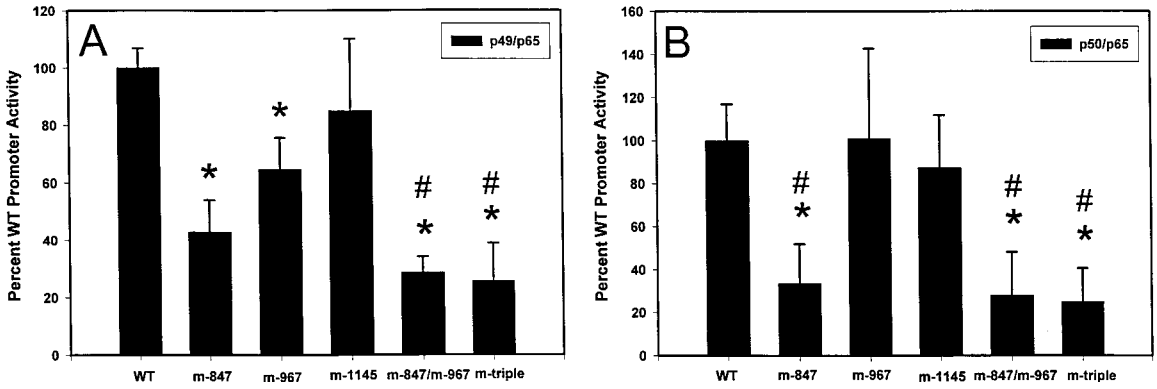

FIG. 7. Promoter activities of the wild-type (WT) 1.1-kb *bcl-x* promoter and mutant 1.1-kb promoters lacking NF-κB binding sites. Promoter activity is expressed as relative light units (RLU) of firefly luciferase activity normalized to RLU of *Renilla* luciferase activity to control for any difference in transfection efficiency. **A:** Promoter activity of the WT and mutant 1.1-kb *bcl-x* promoters during p49/p65 overexpression expressed as percentages of WT promoter activation. Data are mean ± SD (bars) values. Individual groups were composed of individually transfected cultures: WT, n = 32; *bcl-x*-847 mutant, n = 26; *bcl-x*-967 and *bcl-x*-1,145 mutant, n = 22; *bcl-x*-847/-967 mutant, n = 10; *bcl-x*-triple mutant, n = 16. $^{*}p < 0.001$ versus WT, $^{\#}p < 0.05$ versus *bcl-x*-967 and *bcl-x*-1,145. **B:** Promoter activity of WT *bcl-x* and mutant 1.1-kb promoters during p50/p65 overexpression expressed as percentages of WT promoter activation. Data are mean ± SD (bars) values. Individual groups were composed of individually transfected cultures: WT, *bcl-x*-847, *bcl-x*-967, and *bcl-x*-1,145 mutants, n = 28; *bcl-x*-847/-967 and *bcl-x*-triple mutants, n = 16. $^{*}p < 0.001$ versus WT, $^{\#}p < 0.001$ versus *bcl-x*-967 and *bcl-x*-1,145 mutants.

cleotides −1,200 to −600 and containing NF-κB binding sequences is critical for NF-κB-mediated responses.

NF-κB binding sites *bcl-x*-847 and *bcl-x*-967 are important for activation of the *bcl-x* promoter by NF-κB

To establish a direct transcriptional role for the NF-κB binding sites *bcl-x*-847, *bcl-x*-967, and *bcl-x*-1,145, we eliminated each binding site via site-directed mutagenesis within pGL2-1.1. We created three single-site mutants (pGL2-1.1m-847, pGL2-1.1m-967, and pGL2-1.1m-1,145), a double mutant removing the −847 and −967 sites (pGL2-1.1m-847/-967), and the triple mutant (pGL2-1.1m-triple) form of pGL2-1.1 by mutating each site to 5′-AGATCAACT-3′. Each promoter was cotransfected with pRSVp49/pRSVRelA or pRSVp50/pRSV-RelA in addition to pRL-TK, used for transfection normalization. The activity of the wild-type 1.1-kb *bcl-x* promoter was increased three- to fourfold by p49/p65 overexpression and two- to threefold by p50/p65 overexpression, consistent with data shown in Fig. 6 (data not shown). In control groups used to establish baseline promoter activity, the NF-κB expression vectors were replaced by equivalent molar amounts of pRSV-*lacZ*. The activity of the *bcl-x* promoter containing the *bcl-x*-847 binding site mutation averaged 42.9% of wild-type activity following p49/p65 stimulation (Fig. 7A). Similarly, this mutation lowered promoter activity to 33.5% of the wild-type when stimulated by p50/p65 (Fig. 7B). Mutagenesis of the *bcl-x*-967 site caused a less dramatic, but still significant, decrease in p49/p65-mediated promoter activation to 64.6% of the wild-type promoter. The *bcl-x*-967 mutation did not, however, lessen p50/p65-mediated stimulation, which remained 101% of p50/p65-stimulated wild-type control. The activity of the *bcl-x*-1,145 mutant promoter was slightly decreased but not significantly different from the wild-type *bcl-x* promoter following either p49/p65 or p50/p65 stimulation. The promoter containing the double −847/−967 site mutation retained 28.6 and 27.7% of wild-type promoter activity when activated by p49/p65 and p50/p65, respectively. Removal of the *bcl-x*-1,145 site from the double mutant did not result in further loss of promoter activity when activated by either subunit combination. These promoter activation studies establish the importance of the *bcl-x*-847 and *bcl-x*-967 NF-κB binding sites for p49/p65-mediated *bcl-x* promoter activation. The *bcl-x*-847 site alone appears to be critical for activation of the *bcl-x* promoter by p50/p65, suggesting that the *bcl-x* promoter may be subject to regulation by NF-κB via highly specific interactions dependent on DNA sequence and NF-κB subunit composition. That the *bcl-x*-1,145 mutant retained wild-type inducibility after stimulation with either p49/p65 or p50/p65 is consistent with our EMSA and competition data showing that only *bcl-x*-847 and *bcl-x*-967 are capable of strong interactions with NF-κB proteins.

DISCUSSION

The NF-κB/Rel family of transcription factors exists in virtually all cell types but has been best characterized as a mediator of responses to stress, viral and bacterial infection, and injury in the immune system. More recently, it has been shown that NF-κB can also regulate diverse cellular processes such as cell cycle control, oncogenesis, and apoptosis (Waddick and Uckun, 1998; Foo and Nolan, 1999).

There is a growing body of evidence directly implicating the NF-κB/Rel family of transcription factors in the control of apoptosis in the immune and nervous systems. For example, *RelA*(−/−) double knockout mice

demonstrate embryonic lethality due to massive apoptosis of hepatocytes (Beg et al., 1995). Cell lines derived from *relA*(−/−) mice, or those that overexpress a dominant-negative form of IκB-α, show decreased NF-κB binding activity and increased sensitivity to tumor necrosis factor-α-mediated apoptosis (Beg and Baltimore, 1996; Van Antwerp et al., 1996). Treatment of murine B cells and WEHI-231 cells with the antioxidant pyrrolidine dithiocarbamate or *N*-tosyl-L-phenylalanine chloromethyl ketone, IκB-α overexpression, or transforming growth factor-β1, all stimuli that lower NF-κB activity, also results in apoptosis. Apoptosis is blocked in these cells by overexpression of c-Rel or Bcl-x_L (Wu et al., 1996; Sonenshein, 1997). It is clear that NF-κB is important in determining cell fate in the nervous system, although activation of NF-κB causes both pro- and antiapoptotic events. NF-κB neuroprotective against oxidative insults (Lezoualc'h et al., 1998) and β-amyloid toxicity (Barger et al., 1995), but when persistently activated after global ischemia, NF-κB may lead to neuronal death (Clemens et al., 1998). Given such divergent outcomes, it has been suggested that NF-κB activation acts as a checkpoint between cell rescue and apoptosis (Grilli and Memo, 1999).

The NF-κB can affect apoptosis suggests that NF-κB regulates the transcription of genes that are pro- or antiapoptotic determinants. Indeed, the expression of p53, tumor necrosis factor-α, Bcl-2, c-myc, c-IAP1 and 2, IEX-1L, Bfl-1/A1, and FasL is thought to be regulated in part by NF-κB (Collart et al., 1990; Wu and Lozano, 1994; Wang et al., 1998; Wu et al., 1998; Foo and Nolan, 1999).

There is strong evidence to support the hypothesis that the NF-κB regulates *bcl-x* expression. Just how NF-κB affects the *bcl-x* gene is not known. In human B lymphocytes, NF-κB activation via CD40 signaling leads to increased *bcl-x* mRNA and Bcl-x_L protein levels and affords these cells resistance to Fas-mediated apoptosis (Lee et al., 1999). Conversely, wild-type murine thymocytes undergo apoptosis due to NF-κB-mediated decreases in *bcl-*x_L mRNA and Bcl-x_L protein, whereas apoptosis is blocked in transgenic mice expressing the superinhibitory form of IκB-α (Hettmann et al., 1999). In rat hippocampal neurons, NF-κB activation following neuroprotective tumor necrosis factor-α treatment increases *bcl-x* mRNA and protein levels, and viral application of the superinhibitory mutant form of IκB-α blocks this effect (Tamatani et al., 1999). It has also been shown that NF-κB activation correlates with increased proapoptotic Bcl-x_S expression following ischemia in the rat hippocampus in vivo (Dixon et al., 1997).

In this study, we report three primary observations: (a) Computer sequence analysis, EMSA, and competition analysis of *bcl-x* promoter sequences identify two authentic NF-κB binding sites in the murine *bcl-x* promoter. (b) NF-κB activates the murine *bcl-x* promoter in a subunit-specific manner using a NF-κB overexpression model in PC12 cells. (c) Site-directed mutagenesis of the NF-κB binding sites reveals their sequence-specific contributions to *bcl-x* promoter activation.

There are three potential NF-κB sites located at nucleotide positions −1,145, −967, and −847 upstream from the *bcl-x* start codon. The three sites are clustered directly upstream of a brain tissue-specific transcription start site (position −727) and a start site used predominantly in thymus, spleen, and liver (position −655; Fig. 1) (Grillot et al., 1997). Furthermore, two potential NF-κB binding sites corresponding to murine *bcl-x*-967 and *bcl-x*-847 and the brain and thymus-specific start sites are conserved in the human *bcl-x* promoter. This striking similarity of transcriptional element positioning across species supports the notion that NF-κB is important in modulating *bcl-x* expression.

EMSA and competition analysis of the three *bcl-x* NF-κB sequences showed that only the two downstream *bcl-x*-967 and *bcl-x*-847 sequences have measurable affinity for NF-κB under the conditions used (Figs. 2–4 and data not shown). NF-κB activates target gene expression via interaction with a multitude of similar binding sites (Muller et al., 1993), and virtually all homo- and heterodimer subunit combinations of NF-κB have been shown to be present in various different cell types (Liou and Baltimore, 1993). To determine precisely which NF-κB dimer combinations can act on the *bcl-x* promoter, we chose to use a NF-κB expression system to overexpress p49, p50, and p65 alone or in combination. The rat PC12 cell line, often used as an in vitro neuronal model (Greene and Tischler, 1976), was used because it expresses Bcl-x_L (Maroto and Perez-Polo, 1997) and has very low basal nuclear NF-κB binding activity in the absence of stimulation (Fig. 3, lane 1).

The *bcl-x* promoter appears to contain no canonical TATA box, is GC-rich, has numerous consensus sequences for the transcription factor SP-1, and has multiple transcription start sites, all properties of TATA-less promoters (Smale and Baltimore, 1989; Grillot et al., 1997; Smale, 1997). The murine *bcl-x* promoter has been described as having two distinct promoter regions, with transcription start sites mapping to nucleotides −400, −655, and −727 from the ATG in the upstream promoter region and −83 and −96 for the downstream promoter region. The DNA sequences containing these start sites are identical between mouse and human promoters. Initial 5′ deletion analysis of the murine *bcl-x* promoter via transient transfection in human K562 and mouse FL5.12 cells suggested that virtually all of the activity of the 3.2-kb promoter region is contained within nucleotides −160 to −90, relative to the ATG. This is consistent with the fact that the cell lines used primarily utilize the −96 start site, although the possible involvement of upstream enhancers with this site is not known (Grillot et al., 1997).

Our findings that the 1.1Right and 0.5Right promoter regions show decreased basal transcriptional activity in PC12 cells (Fig. 6) and K562 cells (data not shown) relative to the 3.2-kb promoter are not surprising given that 5′ deletions often remove those enhancer regions

required for high-level expression, although these data do not support the observations of others (Grillot et al., 1997). Deletion of the upstream 2.0-kb region lowered basal promoter activity but did not eliminate the ability of the 1.1-kb region to respond to NF-κB. Stimulation of the 1.1-kb region by p49/p65, and to a lesser extent p50/p65, did substitute for the removal of the 2.0-kb region. This is consistent with the idea that the upstream 2.0-kb region may contain enhancer sequence elements bound by other factors present in PC12 cells and that the 1.1-kb region of the promoter is generally sensitive to upstream enhancer elements.

We were surprised by the low basal activity displayed by the 0.5Right promoter region, which contains the −400 and −96 transcription start sites. Because this region is devoid of NF-κB sites, it could not be activated by p49/p65 or p50/p65 overexpression. The 0.6Left promoter region, containing two start sites at −727 and −655 and the NF-κB sites, had a basal activity virtually identical to that of the 0.5Right region but could be activated by both p49/p65 and p50/p65 overexpression (Fig. 6). These data suggest that (a) 0.6- and the 0.5-kb regions are interdependent, with neither having significant activity by itself, (b) NF-κB activation of the *bcl-x* promoter occurs exclusively through interactions in the 0.6Left promoter region, and (c) NF-κB-mediated activation of the *bcl-x* promoter occurs, at least in part, through cooperation with one or both of the two transcription initiation sites contained within the 0.6Left region (Figs. 1 and 6). Further study is needed to determine which transcription initiation start sites are used during NF-κB stimulation in the context of the 1.1-kb promoter region.

Some confirmed NF-κB target genes contain multiple functionally active NF-κB binding sites (Collart et al., 1990; Liou and Baltimore, 1993; Appleby et al., 1994). To determine the contribution of each NF-κB binding site in activating the *bcl-x* promoter, we selected the 1.1-kb region of the promoter for site-directed mutagenesis. The wild-type 1.1-kb region was consistently activated by p49/p65 three- to fourfold, and by p50/p65, two- to threefold over control. Mutagenesis of the *bcl-x*-847 NF-κB site profoundly limited p49/p65- and p50/p65-mediated activation (Fig. 7), confirming the importance of this site in mediating NF-κB effects. This result is especially interesting because EMSAs using nuclear extracts from cells overexpressing p49/p65 and p50/p65 showed virtually no NF-κB binding to the *bcl-x*-847 sequence, contrary to our other EMSA results (Figs. 2 and 3). Although possibly a technical artifact, it may be that the *bcl-x*-847 site requires only weak binding to contribute heavily to NF-κB-mediated affects, or additional DNA flanking sequences not present in the short EMSA oligonucleotide used here are required for strong cooperative interactions at this site. It is important to note that the basal activity of the 1.1-kb region of the *bcl-x* promoter is not decreased by any combination of the site-directed mutations (data not shown), indicating that disruption of the NF-κB protein/DNA interaction alone is responsible for decreased promoter activity.

Mutagenic removal of the *bcl-x*-967 site demonstrated that this site contributes to promoter activation in a subunit-specific manner, favoring p49/p65 for activation. That the *bcl-x*-967 site does not significantly contribute to p50/p65-mediated activation may explain the consistently lower wild-type promoter activation we observe with p50/p65 versus p49/p65. We find this result puzzling in the light of our binding data showing this site's relatively strong interaction with NF-κB proteins, including p49/p65 and p50/p65 from transfected cells. Because our NF-κB-dependent control vector was activated by p50/p65 fourfold (Fig. 5A), we postulate that p50/p65 cannot consistently activate the *bcl-x* promoter through the *bcl-x*-967 site. It is a well-known feature of NF-κB signaling that functionally distinct DNA binding sites exist to which certain NF-κB dimer species preferentially bind. Others have made observations similar to ours in that binding by EMSA does not equate to transcriptional activation of a heterologous promoter in a transfected cell system and that p49/p65 and p50/p65 manifest different effects on target genes bearing nonidentical binding sites, despite the structural similarity of NF-κB p49/p65 and p50/p65 heterodimers (Cross et al., 1989; Liou and Baltimore, 1993). The *bcl-x*-1,145 single mutant displayed wild-type activation by both p49/p65 and p50/p65 overexpression. That the *bcl-x*-1,145 site does not significantly contribute to promoter activation by NF-κB is in accordance with our binding data showing that this site interacts very weakly with NF-κB proteins (Fig. 7). Overall, our mutagenesis data confirm the importance of the *bcl-x*-847 and *bcl-x*-967 NF-κB binding sites of NF-κB-mediated activation of the *bcl-x* promoter.

Mutation of the NF-κB sites alone or in combination had no effect on basal expression levels of the 1.1-kb *bcl-x* promoter/firefly luciferase hybrid reporter vector (data not shown). Although this finding certainly does not rule out a role for NF-κB in modulating basal promoter activity, it suggests that p49/p65 and/or p50/p65-mediated activation for this promoter may be limited to situations that require induced NF-κB activity, such as oxidative stress due to trauma or disease. Different combinations of transcription factors within a single promoter may contribute to gene regulation by integrating multiple signaling pathways. NF-κB often mediates its effects via synergy with other transcription factors, including AP-1, SP-1, and the Ets family of proteins (Mackman et al., 1991; Perkins et al., 1993, 1994; Bassuk et al., 1997; Thomas et al., 1997; Sweet et al., 1998). Binding sites for these factors and others exist within the *bcl-x* promoter (Fig. 1) (Grillot et al., 1997; Sevilla et al., 1999), but functional interaction between these factors and NF-κB remains to be established for *bcl-x* promoter regulation.

In summary, we demonstrate a mechanistic link between two key apoptotic modulators known to influence cell death in the CNS. The murine *bcl-x* promoter can be

activated in a subunit-dependent manner by p49/p65 and p50/p65 subunit combinations of NF-κB. This activation occurs through direct protein–DNA interaction with at least two functionally distinct NF-κB binding sites. Taken together, our results suggest a direct role for NF-κB in the regulation of *bcl-x*. Further attention needs to be focused on defining the role of NF-κB in regulating *bcl-x* and other effector target genes in various paradigms in which NF-κB activation is either pro- or anti-apoptotic. At this time, however, little is known about how NF-κB signaling is integrated into a fate-determining cellular program. Any future use of effective interventions against neurodegenerative disease and injury targeting NF-κB signaling will rely on a full understanding of the role of cell type, NF-κB subunit composition, and target gene function and promoter sensitivity to NF-κB to expand our understanding of apoptosis in the CNS.

Acknowledgment: The authors would like to thank Tracy Toliver-Kinsky, Norbert K. Herzog, Susan Fennewald, and Giulio Taglialatela for critical review of the manuscript and helpful discussion. We gratefully acknowledge Gabriel Nuñez for the gift of the *bcl-x* promoter vectors, Dean Ballard for the pCMV4-IκB-α expression vector, E. Aubrey Thompson for the pRL-TK vector, and Norbert K. Herzog for the 70Z/3 nuclear extracts. This work was supported by grant NS33288 from the National Institute of Neurological Disorders and Stroke, grant 8540 from the Shriner's Burns Institute, and a grant from the Spinal Cord Research Foundation.

REFERENCES

Appleby S., Ristimaki A., Neilson K., Norko K., and Hla T. (1994) Structure of the cyclo-oxygenase-2 gene. *Biochem. J.* **302,** 723–727.

Barger S., Horster D., Furukawa K., Goodman Y., Krieglstein J., and Mattson M. (1995) Tumor necrosis factors alpha and beta protect neurons against amyloid beta-peptide toxicity: evidence for involvement of a kappa B-binding factor and attenuation of peroxide and calcium accumulation. *Proc. Natl. Acad. Sci. USA* **92,** 9328–9332.

Bassuk A., Anandappa R., and Leiden J. (1997) Physical interactions between Ets and NF-kappa B/NFAT proteins play an important role in their cooperative activation of the human immunodeficiency virus enhancer in T cells. *J. Virol.* **71,** 3563–3573.

Beg A. and Baltimore D. (1996) An essential role for NF-kappa B in preventing TNF-alpha-induced cell death. *Science* **274,** 782–784.

Beg A., Sha W., Bronson R., Ghosh S., and Baltimore D. (1995) Embryonic lethality and liver degeneration in mice lacking the RelA component of NF-kappa B. *Nature* **376,** 167–170.

Boise L., Gonzalez-Garcia M., Postema C., Ding L., Lindsten T., Turka L., Mao X., Nunez G., and Thompson C. (1993) Bcl-x, a bcl-2-related gene that functions as a dominant regulator of apoptotic cell death. *Cell* **74,** 597–608.

Brockman J., Scherer D., McKinsey T., Hall S., Qi X., Lee W., and Ballard D. (1995) Coupling of a signal response domain in I kappa B-alpha to multiple pathways for NF-kappa B activation. *Mol. Cell. Biol.* **15,** 2809–2818.

Chen J., Graham S., Nakayama M., Zhu R., Jin K., Stetler R., and Simon R. (1997) Apoptosis repressor genes Bcl-2 and Bcl-x-long are expressed in the rat brain following global ischemia. *J. Cereb. Blood Flow Metab.* **17,** 2–10.

Cheng E., Kirsch D., Clem R., Ravi R., Kastan M., Bedi A., Ueno K., and Hardwick J. (1997) Conversion of Bcl-2 to a Bax-like death effector by caspases. *Science* **278,** 1966–1968.

Cleary M., Smith S., and Sklar J. (1986) Cloning and structural analysis of cDNAs for bcl-2, and a hybrid bcl-2/immunoglobulin transcript resulting from the t(14;18) translocation. *Cell* **47,** 19–28.

Clemens J., Stephenson D., Yin T., Smalstig E., Panetta J., and Little S. (1998) Drug-induced neuroprotection from global ischemia is associated with prevention of persistent but not transient activation of nuclear factor kappa B in rats. *Stroke* **29,** 677–682.

Collart M., Baeuerle P., and Vassalli P. (1990) Regulation of tumor necrosis factor alpha transcription in macrophages: involvement of four kappa B-like motifs and of constitutive and inducible forms of NF-kappa B. *Mol. Cell. Biol.* **10,** 1498–1506.

Cross S., Halden N., Lenardo M., and Leonard W. (1989) Functionally distinct NF-kappa B binding sites in the immunoglobulin kappa and IL-2 alpha chain genes. *Science* **244,** 466–469.

Dixon E., Stephenson D., Clemens J., and Little S. (1997) Bcl-Xshort is elevated following severe global ischemia in rat brains. *Brain Res.* **776,** 222–229.

Duckett C., Perkins N., Kowalik T., Schmidt R., Huang E., Baldwin A. S. Jr., and Nabel G. (1993) Dimerization of NF-kappa B2 with RelA (p65) regulates DNA binding, transcriptional activation, and inhibition by an I kappa B-alpha (MAD3). *Mol. Cell. Biol.* **13,** 1315–1322.

Dyer R. and Herzog N. (1995) Isolation of intact nuclei for nuclear extract preparation from a fragile B-lymphocyte cell line. *Biotechniques* **19,** 192–195.

Foo S. and Nolan G. (1999) NF-kappaB to the rescue: RELs, apoptosis, and cellular transformation. *Trends Genet.* **15,** 229–235.

Frankowski H., Misotten M., Fernandez P.-A., Martinou I., Michel P., Sadoul R., and Martinou J.-C. (1995) Function and expression of the Bcl-x gene in the developing and adult nervous system. *Neuroreport* **6,** 1917–1921.

Fujio Y., Kunisada K., Hirota H., Yamaguchi-Takihara K., and Kishimoto T. (1997) Signals through gp130 upregulate bcl-x gene expression via STAT1-binding cis-element in cardiac myocytes. *J. Clin. Invest.* **99,** 2898–2905.

Gibson L., Holmgreen S., Huang D., Bernard O., Copeland N., Jenkins N., Sutherland G., Baker E., Adams J., and Cory S. (1996) bcl-w, a novel member of the bcl-2 family, promotes cell survival. *Oncogene* **13,** 665–675.

Gonzalez-Garcia M., Perez-Ballestero R., Ding L., Duan L., Boise L., Thompson C., and Nunez G. (1994) Bcl-xL is the major bcl-x mRNA form expressed during murine development and its product localizes to mitochondria. *Development* **120,** 3033–3042.

Gonzalez-Garcia M., Garcia I., Ding L., O'Shea S., and Boise L. (1995) bcl-x is expressed in embryonic and postnatal neural tissues and functions to prevent cell death. *Proc. Natl. Acad. Sci. USA* **92,** 4304–4308.

Gorman C., Padmanabhan R., and Howard B. (1983) High efficiency DNA-mediated transformation of primate cells. *Science* **221,** 551–553.

Greene L. and Tischler A. (1976) Establishment of a noradrenergic clonal line of rat adrenal pheochromocytoma cells which respond to nerve growth factor. *Proc. Natl. Acad. Sci. USA* **73,** 2424–2428.

Gregory T., Channing Y., Ma A., Orkin S., Blobel G., and Weiss M. (1999) GATA-1 and erythropoietin cooperate to promote erythroid cell survival by regulating bcl-XL expression. *Blood* **94,** 87–96.

Grilli M. and Memo M. (1999) Nuclear factor kappa B/Rel proteins: a point of convergence of signalling pathways relevant in neuronal function and dysfunction. *Biochem. Pharmacol.* **57,** 1–7.

Grillot D., Gonzalez-Garcia M., Ekhterae D., Duan L., Inohara N., Ohta S., Seldin M., and Nunez G. (1997) Genomic organization, promoter analysis, and chromosome localization of the mouse bcl-x gene. *J. Immunol.* **158,** 4750–4757.

Gross A., Yin X.-M., Wang K., Wei M., Jockel J., Milliman C., Erdjument-Bromage H., Tempst P., and Korsmeyer S. (1999) Caspase cleaved BID targets mitochondria and is required for cytochrome c release, while Bcl-xL prevents this release but not tumor necrosis factor-R1/Fas death. *J. Biol. Chem.* **274,** 1156–1163.

Hettmann T., DiDonato J., Karin M., and Leiden J. (1999) An essential role for nuclear factor kappa B in promoting double positive thymocyte apoptosis. *J. Exp. Med.* **189,** 145–158.

Hsu Y.-T., Wolter K., and Youle R. (1997) Cytosol-to-membrane redistribution of Bax and Bcl-xL during apoptosis. *Proc. Natl. Acad. Sci. USA* **94,** 3668–3672.

Ito T., Deng X., Carr B., and May W. (1997) Bcl-2 phosphorylation required for anti-apoptosis function. *J. Biol. Chem.* **272,** 11671–11673.

Lee H., Dadgostar H., Cheng Q., Shu J., and Cheng G. (1999) NF-kappa B mediated up-regulation of Bcl-x and Bfl-1/A1 is required for CD40 survival signaling in B lymphocytes. *Proc. Natl. Acad. Sci. USA* **96,** 9136–9141.

Lenardo M., Kuang A., Gifford A., and Baltimore D. (1989) Purified bovine NF-kappa B recognizes regulatory sequences in multiple genes expressed during activation of T- and B-lymphocytes. *Hamatol. Bluttransfus.* **32,** 411–415.

Lezoualc'h F., Sagara Y., Holsboer F., and Behl C. (1998) High constitutive NF-kappa B activity mediates resistance to oxidative stress in neuronal cells. *J. Neurosci.* **18,** 3224–3232.

Lin R., Gewert D., and Hiscott J. (1995) Differential transcriptional activation in vitro by NF-kappa B/Rel proteins. *J. Biol. Chem.* **270,** 3123–3131.

Liou H.-C. and Baltimore D. (1993) Regulation of the NF-kappa B/rel transcription factor and I kappa B inhibitor system. *Curr. Opin. Cell Biol.* **5,** 477–487.

Liou H.-C., Sha W., Scott M., and Baltimore D. (1994) Sequential induction of NF-kappa B/Rel family proteins during B-cell terminal differentiation. *Mol. Cell. Biol.* **14,** 5349–5359.

Mackman N., Brand K., and Edgington T. (1991) Lipopolysaccharide-mediated transcriptional activation of the human tissue factor gene in THP-1 monocytic cells requires both activator protein 1 and nuclear factor kappa B binding sites. *J. Exp. Med.* **174,** 1517–1526.

Maroto R. and Perez-Polo J. (1997) Bcl-2 related protein expression in apoptosis: oxidative stress versus serum deprivation in PC12 cells. *J. Neurochem.* **69,** 514–523.

Michaelidis T., Sendtner M., Cooper J., Airaksinen M., Holtmann B., Meyer M., and Thoenen H. (1996) Inactivation of bcl-2 results in progressive degeneration of motoneurons, sympathetic and sensory neurons during early postnatal development. *Neuron* **17,** 75–89.

Mitchell D., Vaughan J., and Nairn R. (1989) Inhibition of transient gene expression in Chinese hamster ovary cells by cyclobutane dimers and (6-4) photoproducts in transfected ultraviolet-irradiated plasmid DNA. *Plasmid* **21,** 21–30.

Motoyama N., Wang F., Roth K., Sawa H., and Nakayama K.-I. (1995) Massive cell death of immature hematopoietic cells and neurons in Bcl-x-deficient mice. *Science* **267,** 1506–1510.

Muller J., Ziegler-Heitbrock H., and Baeuerle P. (1993) Nuclear factor kappa B, a mediator of lipopolysaccharide effects. *Immunobiology* **187,** 233–256.

O'Neill L. and Kaltschmidt C. (1997) NF-kappa B: a crucial transcription factor for glial and neuronal cell function. *Trends Neurosci.* **20,** 252–258.

Oppenheim R. (1991) Cell death during development of the nervous system. *Annu. Rev. Neurosci.* **14,** 453–501.

Parsadanian A., Cheng Y., Keller-Peck C., Holtzman D., and Snider W. (1998) Bcl-xL is an antiapoptotic regulator for postnatal CNS neurons. *J. Neurosci.* **18,** 1009–1019.

Perkins N., Schmid R., Duckett C., Leung K., Rice N., and Nabel G. (1992) Distinct combinations of NF-kappa B subunits determine the specificity of transcriptional activation. *Proc. Natl. Acad. Sci. USA* **89,** 1529–1533.

Perkins N., Edwards N., Duckett C., Agranoff A., Schmid R., and Nabel G. (1993) A cooperative interaction between NF-kappa B and Sp-1 is required for HIV-1 enhancer activation. *EMBO J.* **12,** 3551–3558.

Perkins N., Agranoff A., Pascal E., and Nabel J. (1994) An interaction between DNA binding-domains of RelAp65 and Sp-1 mediates human immunodeficiency virus activation. *Mol. Cell. Biol.* **14,** 6570–6583.

Raff M. (1992) Social controls on cell survival and cell death. *Nature* **356,** 397–400.

Schmid R., Perkins N., Duckett C., Andrews P., and Nabel G. (1991) Cloning of an NF-kappa B subunit which stimulates HIV transcription in synergy with p65. *Nature* **352,** 733–736.

Sen R. and Baltimore D. (1986) Multiple nuclear factors interact with the immunoglobulin enhancer sequences. *Cell* **46,** 705–716.

Sevilla L., Aperlo C., Dulic V., Chambard J., Boutonnet C., Pasquier O., Pognonec P., and Boulukos K. (1999) The Ets2 transcription factor inhibits apoptosis induced by colony-stimulating factor 1 deprivation of macrophages through a Bcl-xL-dependent mechanism. *Mol. Cell. Biol.* **19,** 2624–2634.

Silva M., Benito A., Sanz C., Prosper F., Ekhterae D., Nunez G., and Fernandez-Luna J. (1999) Erythropoietin can induce the expression of Bcl-XL through Stat5 in erythropoietin-dependent progenitor cell lines. *J. Biol. Chem.* **274,** 22165–22169.

Smale S. (1997) Transcription initiation from TATA-less promoters within eukaryotic protein coding genes. *Biochim. Biophys. Acta* **1351,** 73–88.

Smale S. and Baltimore D. (1989) The "Initiator" as a transcription control element. *Cell* **57,** 103–113.

Sonenshein G. (1997) Rel/NF-kappa B transcription factors and the control of apoptosis. *Semin. Cancer Biol.* **8,** 113–119.

Sweet M., Stacey K., Ross I., Ostrowski M., and Hume D. (1998) Involvement of Ets, rel, and Sp-1-like proteins in lipopolysaccharide-mediated activation of the HIV-1 LTR in macrophages. *J. Inflamm.* **48,** 67–83.

Tamatani M., Che Y., Matsuzaki H., Ogawa S., Okado H., Miyake S., Mizuno T., and Tohyama M. (1999) Tumor necrosis factor induces Bcl-2 and Bcl-x expression through NF-kappa B activation in primary hippocampal neurons. *J. Biol. Chem.* **274,** 8531–8538.

Thomas R., Tymms M., McKinlay L., Shannon M., Seth A., and Kola I. (1997) ETS1, NFkappaB and AP1 synergistically transactivate the human GM-CSF promoter. *Oncogene* **14,** 2845–2855.

Tsujimoto Y. and Croce C. (1986) Analysis of the structure, transcripts, and protein products of bcl-2, the gene involved in human follicular lymphoma. *Proc. Natl. Acad. Sci. USA* **83,** 5214–5218.

Van Antwerp D., Martin D., Kafri T., Green D., and Verma I. (1996) Suppression of TNF-alpha-induced apoptosis by NF-kappa B. *Science* **274,** 787–789.

Waddick K. and Uckun F. (1998) Innovative treatment programs against cancer. *Biochem. Pharmacol.* **57,** 9–17.

Wang C.-Y., Mayo M., Korneluk R., Goeddel D., and Baldwin A. (1998) NF-kappaB antiapoptosis: induction of TRAF1 and TRAF2 and c-IAP1 and c-IAP2 to suppress caspase-8 activation. *Science* **281,** 1680–1683.

Whiteside S. and Israel A. (1997) I kappa B proteins: structure, function and regulation. *Semin. Cancer Biol.* **8,** 75–82.

Wolter K., Hsu Y., Smith C., Nechushtan A., Xi X., and Youle R. (1997) Movement of Bax from the cytosol to the mitochondria during apoptosis. *J. Cell Biol.* **139,** 1281–1292.

Wu H. and Lozano G. (1994) NF-kappa B activation of p53. A potential mechanism for suppressing cell growth in response to stress. *J. Biol. Chem.* **269,** 20067–20074.

Wu M., Lee H., Bellas R., Schauer S., Arsura M., Katz D., Fitzgerald M., Rothstein T., Sherr D., and Sonenshein G. (1996) Inhibition of NF-kappaB/Rel induces apoptosis of murine B cells. *EMBO J.* **15,** 4682–4690.

Wu M., Ao Z., Prasad K., Wu R., and Schlossman S. (1998) IEX-1L, an apoptosis inhibitor involved in NF-kappa B-mediated cell survival. *Science* **281,** 998–1001.

Yang E., Zha J., Jockel J., Boise L., Thompson C., and Korsmeyer S. (1995) Bad, a heterodimeric partner of Bcl-xL and Bcl-2, displaces Bax and promotes cell death. *Cell* **80,** 285–291.

Zha J., Harada H., Yang E., Jockel J., and Korsmeyer S. (1996) Serine phosphorylation of death agonist BAD in response to survival factor results in binding to 14-3-3- not Bcl-xL. *Cell* **87,** 619–628.